

Short communication

Electrochemical behavior of the polypyrrole/polyimide composite by potential step amperometry

Kirill L. Levine¹, Jude O. Iroh*

Chemical Engineering and Materials Science Department, University of Cincinnati, Cincinnati, OH 45221-0012, USA

Received 29 April 2003; accepted 19 May 2003

Abstract

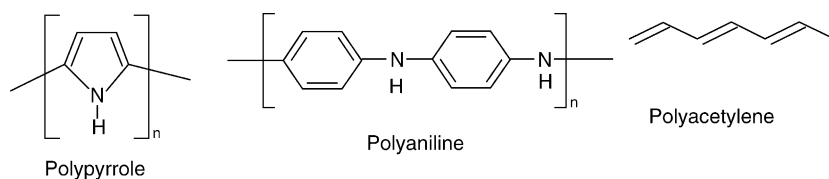
A polypyrrole (PPy)/polyimide (PI) composite was prepared electrochemically in order to improve the mechanical and electrochemical properties of PPy. The electrochemical behavior of the composite was studied by potential step amperometry. The composites were found to possess increased charge storage ability in comparison to pure PPy. It was found that the doping of PPy by PI is responsible for the increased charge storage ability of the composite.

© 2003 Elsevier B.V. All rights reserved.

Keywords: Polypyrrole; Polyimide; Composite; Conducting polymers; Potential step amperometry

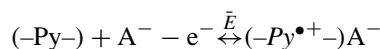
1. Introduction

Intrinsically conducting polymers (ICPs) are a class of polymers that contain conjugated double bonds. Examples of ICPs are: polypyrrole (PPy), polyaniline (PANI) and polyacetylene.

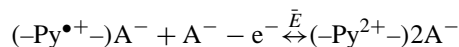


Due to their electroactivity and high surface area, ICPs are being evaluated for practical applications in polymer batteries [1,2] and supercapacitors [3–6]. However, poor mechanical properties and low environmental stability of pure ICPs remain a serious obstacle to their practical application. One of the ways to solve this problem is to formulate the composites composed of the ICP filler and a polymeric matrix with attractive mechanical properties. In this paper, polyimide (PI) was used as a matrix for a composite with ICP, because of its excellent thermal stability and

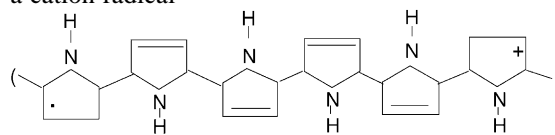
very good mechanical properties. PPy was chosen as a filler because of its relatively good environmental stability and electroactivity. Electroactivity of PPy can be represented as follows:



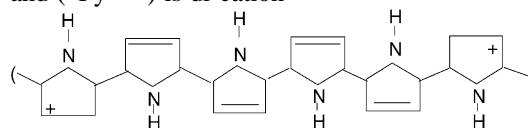
and



where $(-\text{Py}-)$ are pyrrole monomers (above), $(-\text{Py}^{\bullet+}-)$ is a cation radical



and $(-\text{Py}^{2+}-)$ is di-cation



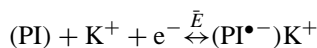
A composite comprised of PPy filler and PI matrix can be prepared electrochemically [7–9]. In the PPy/PI composite, the matrix protects PPy from oxidation by oxygen [10]. An

* Corresponding author. Tel.: +1-513-556-3115.

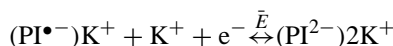
E-mail addresses: kirill.levine@ndsu.nodak.edu (K.L. Levine), irohj@email.uc.edu (J.O. Iroh).

¹ Present address: Department of Polymers and Coatings, 1735 NDSU Research Park Drive, North Dakota State University, Polymer and Coatings, 58105, Fargo, ND, USA.

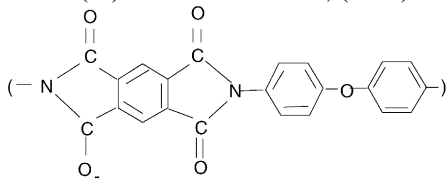
additional consideration for choosing PI as a matrix for the composite with PPy is the electroactivity of PI [11]:



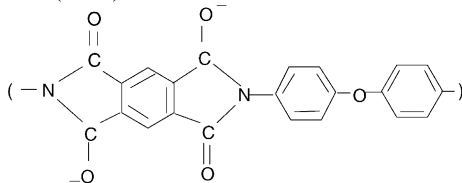
and



where (PI) is a monomer unit, (PI^{•−}) is an anion radical:



and (PI^{2−}) is di-anion



The electrochemical formation of anion radicals takes place in the first step, and the di-anion forms in the second step. Electroneutrality is maintained by counter ions. Charge storage properties of the PPy/PI composite are mainly due to doping/dedoping of PPy in the presence of the electroactive PI matrix [12]. Pseudocapacitance (capacitance that is due to doping/dedoping) was recently studied by electrochemical impedance spectroscopy (EIS). It was shown that the pseudocapacitance of the PPy/PI composite changes with changing dc polarization potential because of the changed level of doping [12]. It was also shown that pseudocapacitance of the composite increases with the increased amount of PPy and reaches 40 mC/cm² when the time of PPy deposition is 400 s. However, at low frequencies (less than 0.05 Hz) EIS results can be affected by polarization currents. Potential step amperometry (PSA) allows the determination of the charge storage ability directly, by integrating the area under the discharge curve. In this paper, PSA was used to study the discharge behavior of pure PPy and the PPy/PI composites for application to polymer-based charge storage systems.

2. Experimental

2.1. Apparatus

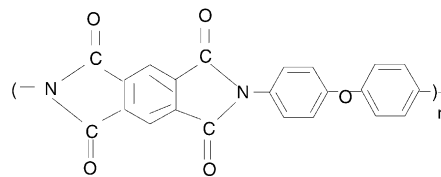
Fourier transform infrared spectroscopy (FTIR) was performed by using a BIO-RAD FTS-40 FTIR spectrometer. The morphology of the composites was examined by a Hitachi S-4000 scanning electron microscope (SEM). The SEM samples were sputtered with gold to improve conductivity.

The electrodeposition of PPy and PSA experiments were performed with a EG & G Potentiostat-Galvanostat model 273 A.

2.2. Methods

2.2.1. Samples preparation

A solution of poly(amic acid) resin² (28% in *N*-methylpyrrolidinone (NMP)) purchased from DuPont Electronics was diluted to 10% by dimethylacetamide (DMAc). The PAAc solution was cast onto a stainless steel (SS) working electrode and subsequently dried at 70 °C for 1 h to form a film of 15–20 μm thickness. A PAAc film formed on SS steel was converted to PI by chemical imidization, as described by Koton et al. [13]. The molecular structure of PI after imidization is shown above. Electrodeposition of PPy on PI-coated electrode was carried out galvanostatically in a solution containing 0.01 M pyrrole (Py)³ and 0.1 M potassium hexafluorophosphate (KPF₆) in acetonitrile (AN), by the same procedure as in [12]. A current density of 1 mA/cm² was applied until the desired amount of charge was consumed. A single-compartment electrochemical cell was used for the experiments. The electrochemical cell was composed of the PI-coated SS working electrode, SS counter electrode and a saturated calomel reference electrode⁴ (SCE). During the electrochemical polymerization of Py onto the PI covered SS electrode, the PPy/PI composite was formed. The resulting PPy/PI films were firmly bonded to the surface of the working electrode. After electrodeposition was completed, the composite film was dedoped and discharged by short-circuiting the counter and working electrode for 5 min in monomer-free solution. During discharging, the current between working electrode and counter electrode decreased from the milliamperes to the nanoampere range. After discharging was completed, the films were rinsed in AN for 10 min.



Pyromellitic Dianhydride 4,4'-oxydianiline

FTIR spectra showed that the amount of PPy in the composite increased with the increasing time of deposition (Fig. 1). The relative intensity of the PPy characteristic peak (C–H in pyrrole ring) at 1050 cm^{−1} is plotted as a function of the calculated amount of PPy based on electrodeposition time. The IR peak occurring at 1015 cm^{−1} is associated

² Pyromellitic dianhydride 4,4'-oxydianiline was used.

³ Monomer, solvent and chemicals were used Aldrich grade without further purification.

⁴ All the potentials were applied versus SCE.

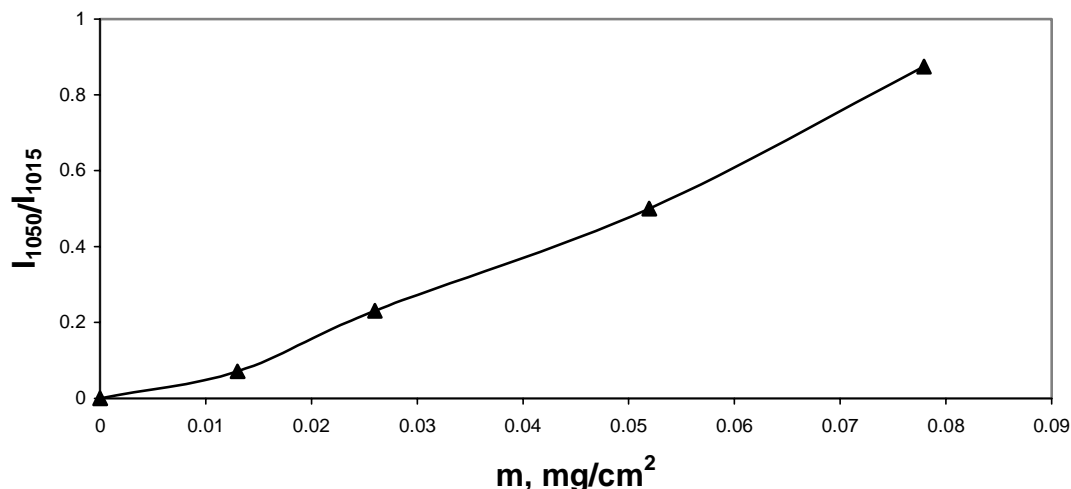


Fig. 1. Relative intensity of 1050 cm^{-1} peak as a function of amount of PPy in the PPy/PI composite.

with the vibration of the phenyl ring present in PI and was used as a standard.

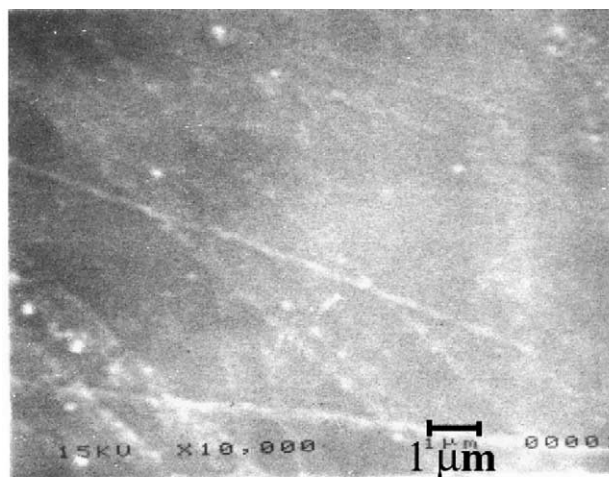
2.2.2. Potential step amperometry

Charging of films was carried out potentiostatically. An anodic charging potential (E_{ch}) in the range of 0.5–2.1 V was applied to charge films during a charging time (t_1). Immediately after charging was completed, films were switched to a discharging potential (E_{dch}) equal to 0.0 V that was close to the open circuit potential within ± 10 mV. The discharging current was monitored as a function of discharging time (t_2). Evaluation of the area under $\log I$ versus t_2 curve was done to determine the charge passed.

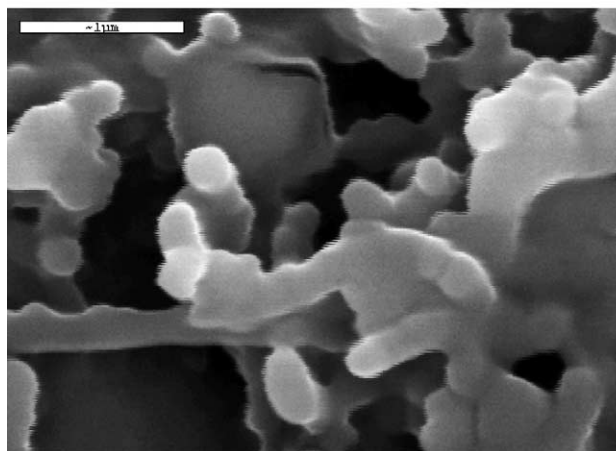
3. Results and discussion

The morphology of the composite film shows the presence of PPy. Fig. 2 shows the SEM picture for the PPy/PI composite. Pure PI film has a smooth surface morphology (Fig. 2A), while deposition of PPy causes roughening. Filaments shown in Fig. 2B possibly contain increased amounts of PPy.

Potential step measurements were performed on an uncoated SS electrode, PI-coated SS electrode, PPy-coated SS and PPy/PI-composite-coated SS at different charging times and potentials. The discharge behavior of the bare electrode and pure PI films are shown in Fig. 3. The discharge process shown on a bare electrode is associated with the capacitance of a double electric layer (DEL) at the electrode/solution interface. The DEL is composed of a positively charged metal surface and negatively charged hexafluorophosphate ions. As shown in Fig. 3, the discharge current for the PI film exceeds that for a bare electrode by about one order of magnitude. In this case, highly polarizable PI molecules are responsible for the increase in the capacitance of the composite. The pseudocapacitance of the PPy film is an addi-



(A)



(B)

Fig. 2. SEM images of pure PI film and the PPy/PI composite: (A) pure PI; (B) the PPy/PI composite; (bottom) 500 s of PPy deposition.

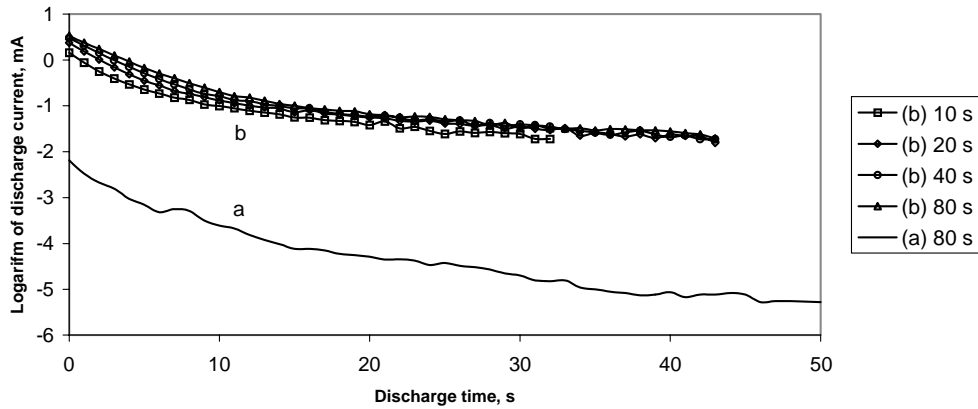


Fig. 3. Discharging behavior of the electrochemical cell with: (a) bare electrode ($t_1 = 10, 20, 40, 80$ s); (b) PI film ($t_1 = 80$ s), $U_{ch} = 1.1$ V.

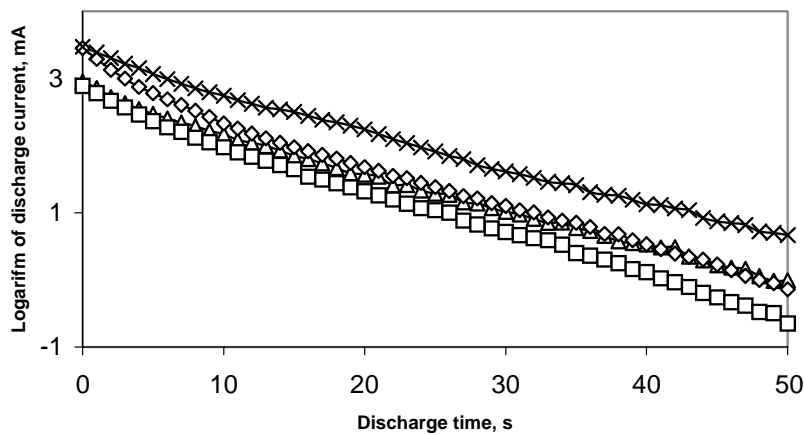


Fig. 4. Discharge behavior of PPy film ($t_1 = 10$ s (\square), $t_1 = 20$ s (Δ), $t_1 = 40$ s (\diamond), $t_1 = 80$ s (\times); $E_{ch} = 1.1$ V).

tional mechanism that contributes to the discharge current (Fig. 4). A linear dependence for the discharge of PPy on steel is shown in a time–current curve. The equivalent circuit model for this approximation includes the capacitance of the film C_{film} that is in parallel with film resistance R_{po} . R_s is the solution resistance. This equivalent circuit model predicts a linear dependence of the logarithm of discharge current on discharge time.

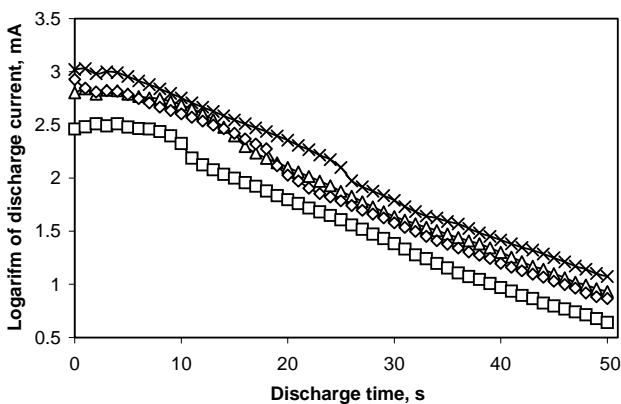
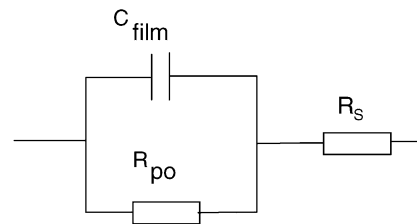


Fig. 5. Discharge behavior of the PPy/PI composite ($t_1 = 10$ s (\square), $t_1 = 20$ s (Δ), $t_1 = 40$ s (\diamond), $t_1 = 80$ s (\times); $E_{ch} = 1.1$ V).

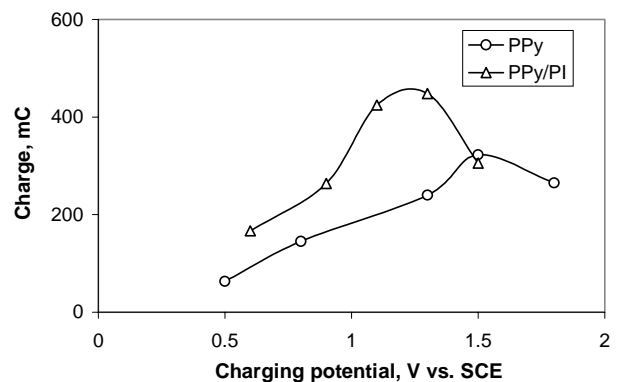


Fig. 6. Dependence of charge Q_{dch} on charging potential E_{ch} . Charging time 50 s. Electrode area 10 cm^2 .

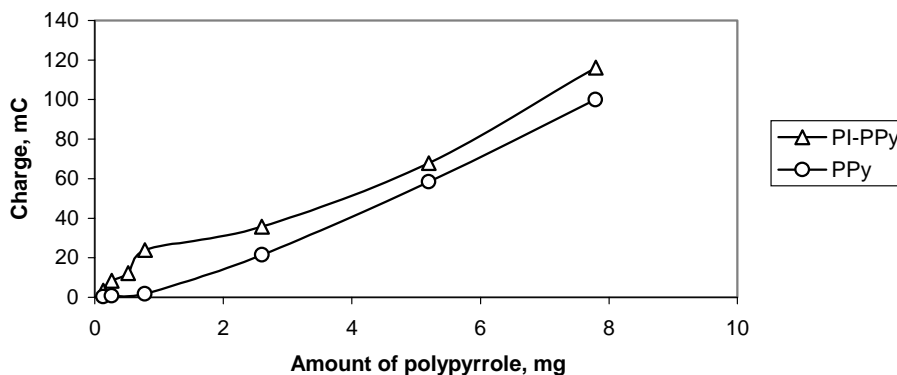
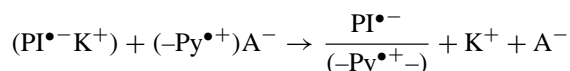


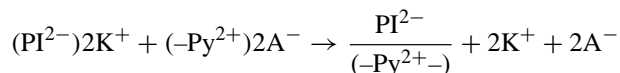
Fig. 7. Dependence of charge Q_{dch} on the amount of PPy. Charging time 50 s. Electrode area 10 cm^2 .

In the case of the PPy/PI composite, $\log(I)$ versus t_2 curve shows two types of behavior (Fig. 5). The behavior at long discharge time is linear and is similar to the previous case. The behavior for short discharge time deviates from linear behavior. The magnitude of the discharge current in the case of the composite is significantly larger possibly because of the effect of discharge of the PPy/PI complexes.

The nature of the interaction between PPy and PI can be represented:



or



It is noted that a significant spin signal was observed in the PPy/PI composite [10]. Consequently, there is a significant amount of non-interacting ion radicals in the composite (not shown in the reaction above).

A plot of the electric charge released by a charged film to the internal electric circuit (Q_{dch}) as a function of charging potential (E_{ch}) is shown in Fig. 6. This dependence resembles a bell shape. The charge storage ability of the PPy/PI composite obtained from Fig. 6 is around 20 mF/cm^2 at potential 1 V. This is in agreement with the data obtained by EIS [12]. Values obtained by EIS were found to be higher, possibly because of the influence of dc polarization currents.

The dependence of the charge on the amount of PPy is shown in Fig. 7. The charge accumulation increases with the increased amount of PPy. Q_{dch} values for the PPy/PI composite are shown to be larger than that for pure PPy. The behavior observed in Figs. 6 and 7 is possibly due to protection of PPy from overoxidation by PI and doping of PPy by PI.

4. Conclusions

Potential step amperometry was used to characterize the electrochemical behavior of the PPy/PI composite prepared by electrochemical deposition of PPy on to PI-coated stain-

less steel. A significant difference between the behavior of PPy-coated SS, bare SS and the PPy/PI-composite-coated SS was observed. This behavior is believed to be due to the pseudocapacitance of PPy and the additional doping provided by the PI matrix. The PI matrix also protects PPy from overoxidation and results in increased charge storage ability. The pseudocapacitance of the PPy/PI composite obtained by PSA is in agreement with that obtained by EIS.

Acknowledgements

Authors are grateful to National Science Foundation DMR for financial support.

References

- [1] E. Spila, S. Panero, B. Scrosati, Solid-state dion battery, *Electrochim. Acta* 43 (10) (1998) 1651–1653.
- [2] D. Delabouglise, Dispersed polypyrrole latex as a cathode material for all-solid-state lithium batteries, *J. Chem. Phys.* 92 (1995) 2048–2059.
- [3] M. Satoh, H. Ishikawa, K. Amano, E. Hasegawa, K. Yoshino, *Synth. Met.* 71 (1995) 2259–2260.
- [4] C. Arbizzani, M. Mastragostino, L. Meneghello, *Electrochim. Acta* 41 (1) (1996) 21–26.
- [5] S. Panero, P. Prosperi, F. Bonino, B. Scrosati, *Electrochim. Acta* 32 (7) (1987) 1107.
- [6] T. Otero, I. Cantero, *J. Power Sources* 81–82 (1999) 838–841.
- [7] B. Tieke, W. Gabriel, Conducting polypyrrole/polyimide composite films, *Polymer* 30 (1) (1990) 20.
- [8] K. Levin, V. Zgonnic, V. Frolov, Electrochemical obtaining and researching of composite of polypyrrole and polyimid, *Vysokomol. Soedin. B* 35 (10) (1993) 1705.
- [9] F. Selampinar, U. Akbulut, L. Toppare, Conducting polymer composites of polypyrrole and polyimide, *Synth. Met.* 84 (1997) 85.
- [10] K. Levin, T. Borisova, V. Zgonnik, V. Frolov, I. Ushakova, Electron spin resonance study of thermal stability of polypyrrole–polyimide composites, *Polym. Sci. B* 42 (2000) 31–33.
- [11] R. Haushalter, L. Krause, *Thin Solid Films* 102 (1983) 161.
- [12] J. Iroh, K. Levine, Capacitance of polypyrrole/polyimide composite by electrochemical impedance spectroscopy, *J. Power Sources* 117 (1–2) (2003) 267–272.
- [13] M. Koton, V. Kudryavtsev, V. Zubkov, A. Yakimansky, T. Meleshko, N. Bogorad, *Vysokomol. Soedin., A* 26 (1984) 2584.